

A 100dB dynamic range high-speed dual-line optical transient sensor with asynchronous readout

P. Lichtsteiner, T. Delbruck
Institute of Neuroinformatics
ETH/Uni Zürich
Zürich, Switzerland

C. Posch
Neuroinformatik
ARC Seibersdorf research GmbH
Vienna, Austria

Abstract—We present a 100dB dynamic range 2×64 pixel dual-line optical sensor with asynchronous event-based readout. Each individual pixel of the sensor operates autonomously and responds with $<100\mu\text{s}$ latency to relative intensity changes. It operates largely independent of overall scene illumination, directly encodes object reflectance, and greatly reduces redundancy while preserving precise timing information. The line sensor was fabricated using a $0.35\mu\text{m}$ standard CMOS technology. Results of the measurement performance of the sensor are presented. The intended application area is precision timing measurement under variable lighting conditions.

I. INTRODUCTION

Optical line sensors are traditionally used for high-speed imaging problems in industrial applications where the target objects move at controlled speed and under controlled lighting conditions perpendicular to the line of sensor elements. A typical application is quality inspection on a conveyor belt.

Traditional clocked line sensors produce huge amounts of data when employed in high-speed short-latency machine vision problems. For certain applications such as measurement tasks, object classification, object orientation monitoring etc. a large amount of the image data produced do not provide any information necessary to accomplish the function or to increase reliability or precision. One way to suppress redundancy is to use a temporally differentiating event-driven sensor architecture. We propose a pixel circuit that operates autonomously and responds in real-time to relative intensity changes by placing its address on an asynchronous arbitrated bus. Pixels that are not stimulated by a change in illumination do not produce output data. Because there is no pixel readout clock, no time quantization takes place at this point. This type of asynchronous communication is called Address Event Representation (AER) [1].

High-speed imaging usually depends on controlled lighting conditions. The pixel circuit realized in this sensor is able to detect contrast changes of a few percent over a dynamic range of 100dB, from under 1lux to more than

10klux of scene illumination ($f/1.4$ lens), and is thus suitable for use under difficult, variable lighting conditions e.g. road traffic monitoring or surveillance.

Furthermore the dual-line configuration provides additional functionality such as precision measurements of object velocities or trajectory angles by correlating AER streams from the two parallel pixel lines. The sparse data delivered by the sensor require low computational effort and power consumption in the subsequent processing stages and allow for compact and low-cost embedded and mobile systems.

II. SENSOR ARCHITECTURE

A block diagram of the sensor architecture is shown in Fig. 1. 128 pixels are arranged in two parallel lines of 64 at a distance of $240\mu\text{m}$.

The pixels communicate with the row and column arbiters via handshake signals request (RR, CRON, CROFF) and acknowledge (RA, CAON, CAOFF). Row and column addresses are set in the respective encoders and communicated off chip on the 8-bit AER bus (6 bits column address, 1 bit row address, 1 ON/OFF polarity bit).

An external receiver acknowledges successful reception of the event. Pixels signaling simultaneously are serviced sequentially at a sustained event rate of $\approx 2 \cdot 10^6$ events per second, if not limited by a slower receiver.

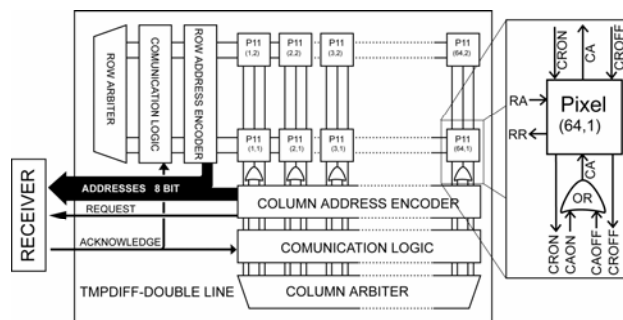


Fig. 1 Block diagram depicting the sensor architecture

TABLE I. contains specifications of the sensor chip.

TABLE I. SPECIFICATIONS OF THE DUAL-LINE SENSOR

Pixel area	1600 μm^2
Pixel complexity	28 transistors (16 analog), 3 capacitors
Biasing requirements	12 generated gate biases
Fabrication process	4-Metal 2-Poly 0.35 μm standard CMOS
Configuration	2 \times 64
Interface	AER, 8-bit address (X, line bit, polarity bit) 4-phase handshake
Dynamic range	> 100dB
Minimum scene illumination using $f/1.4$ lens	$\sim 1\text{mW}/\text{m}^2$ or 1lux.
Photodiode dark current	20fA ($\sim 10\text{nA}/\text{cm}^2$)
Max event rate	> $2 \cdot 10^6$ events per second
System latency	< 100 μs

III. PIXEL OPERATION

A. Temporal Derivative Pixel

The temporal derivative (TMPDIFF) pixel reduces image redundancy by responding only to temporal changes in logarithmic intensity. Static scenes produce no output. Image motion produces spike event output that represents *relative changes in image intensity*. This operation in continuous form is represented mathematically by the operation (1) on the pixel illumination I .

$$\frac{d}{dt} \log I = \frac{dI/dt}{I} \quad (1)$$

This temporal derivative is ‘self-normalized’; the derivative encodes changes in contrast rather than absolute illumination differences. Contrasts are determined by differences in reflectance of objects independent of overall scene illumination. The events generated by TMPDIFF are changes in (1) that exceed a threshold and are ON or OFF type depending on the sign of the change since the last event. Pixel output consists of a stream of ON and OFF events.

B. The Pixel Circuit

The TMPDIFF pixel (Fig. 2) uses the excellent matching between capacitors to form a self clocked switched-capacitor change amplifier. The front-end is an active unity-gain logarithmic photoreceptor that extends bandwidth to low intensities and can be self-biased by the average photocurrent [2].

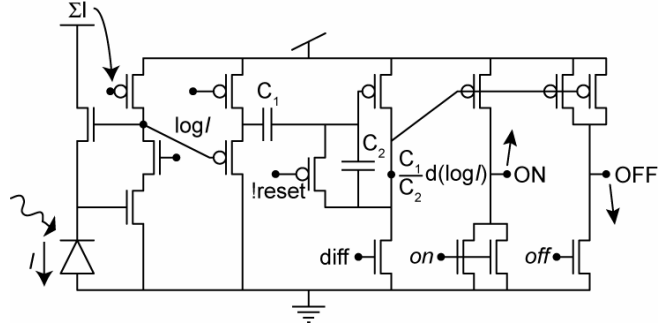


Fig. 2 Pixel circuit. $\log I$ photoreceptor output is buffered to an inverting differentiator, which is reset after each event by the AER communication hand shake. An ON or OFF event is triggered when the differentiator output exceeds the threshold set by *on* and *off*. The globally summed photocurrent can be used to adaptively set the photoreceptor bias.

The photoreceptor is buffered to a voltage-mode capacitive-feedback amplifier with closed-loop gain $A=20$ that is balanced after transmission of each event by the AER handshake. ON and OFF events are detected by the subsequent comparators.

With the pixel circuit in its balanced state (after a reset), ON is clamped near ground and OFF near V_{dd} . If the photocurrent increases by a factor of more than $\exp(\ln(2)/A) \approx 1.05$ (or a change of about 5%), the node ON will go high. Consequently an ON event is initiated with a request to the arbiter. An OFF event happens analogously if the photocurrent decreases by about 5%.

Mismatch of the event threshold is determined by only 5 transistors and is effectively further reduced by the gain of the amplifier. The key to the low FPN is that the mismatch of the event threshold referred to the input (contrast) is reduced by the well matched capacitor loop gain $A=C1/C2$ of the amplifier, e.g. a 10mV comparator mismatch is reduced to 0.5mV at the photosensor, corresponding to a contrast of $\approx 1.75\%$.

IV. RESULTS

A. Time resolution

To measure the response of the line sensor to fast stimuli a 50% gray circular spot on a white background was presented to the sensor. The spot was drawn on a disk in a distances of 9cm from the center. The disk was rotated at variable speeds of up to more than 100 revolutions per second.

Fig. 3 shows the calculated speed of the stimulus image on the sensor focal plane with the disk rotating at 57 revolutions per second. The on-chip speed is a more practical metric than the actual stimulus speed, because the geometrical properties of the setup and parameters of the optical lens have not to be taken into account. The stimulus image spans over about 24 pixels, roughly one third of a line, and moves from right to left with an on-chip speed of 2.9m/s.

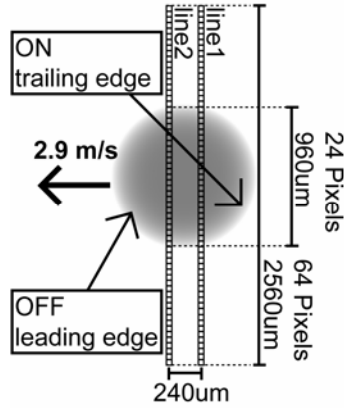


Fig. 3 Gray (50% gray) spot stimulus projected onto the sensor focal plane.

Fig. 4 shows the response of the line sensor to this stimulus at a scene illumination of ≈ 1 klux using a $f/1.4$ lens. The bandwidth of the receiver connected to line sensor limits the output to less than 10^6 events per second. The address events (color and shape coded for the different polarities (ON/OFF) and the two lines) are displayed in the upper plot. A marker represents an event that occurred at a certain time in a certain pixel. The circles depict OFF events, the squares ON events. The data originating from the two lines are distinguished by using empty and filled markers.

The OFF events, representing a transition from higher to lower pixel illumination intensity, track the leading edge of the circular spot and the ON events track its trailing edge. The first OFF event of line 2 appears $91\mu\text{s}$ after the first OFF event of line 1. Within this period, the leading edge shape is still temporally resolved, exhibiting a time resolution of around $10\mu\text{s}$. Effects of limited AE bus bandwidth appear as characteristic patterns of sequential event processing of certain OFF events of the second line and indicate that the sensor combined with the data receiver is operated near its limits. A faster receiver would extend the speed range until the intrinsic limit of the sensor is reached. The sensor is able to deliver address events at a sustained rate of $\approx 2 \cdot 10^6$ events per second.

The lower panels of Fig. 4 show the histograms of activity in time. By measuring the shift in time of the edges of the second line relative to the first line, the speed of the stimulus at the focal plane of the chip can be determined.

Fig. 5 shows a logarithmic plot of speed measured by the sensor versus known stimulus speed. To quantify the speed we measured the time differences between the first OFF events of the first and second line as well as the time differences between the last ON events of both lines (see also Fig. 4 upper panel). The square data points represent measurements with the stimulus moving at different velocities from $\approx 45\text{mm/s}$ to $\approx 3\text{m/s}$ on the sensor plane. The data points are distributed along the line $y = x$. This result indicates that the velocity is reliably represented over a wide range of velocities.

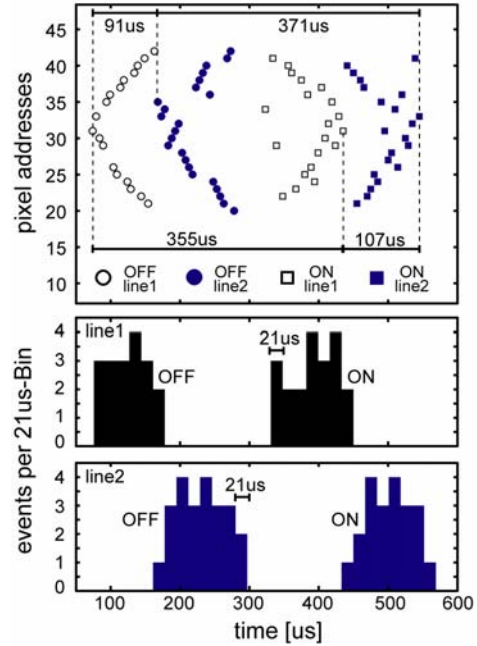


Fig. 4 The events generated in response to the described stimulus. The upper plot shows the individual events and the lower two plots show histograms of ON and OFF events in time for the first line and the second line.

Three data points are labeled and the three corresponding plots on the right show that the event distribution looks very similar for speeds that are about two orders of magnitude apart. For very slow velocities, each pixel produces several events for a single stimulus edge. A simple correlation method applied to the address event data of the two lines can be used to precisely determine the delta time. This task can be performed in a straightforward way by a simple, inexpensive DSP.

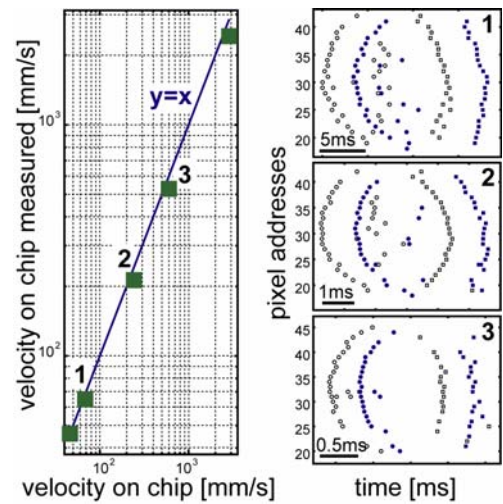


Fig. 5 Velocity measurements for different stimulus speeds plotted on a logarithmic scale and the corresponding events of the three labeled data points.

B. Dynamic range

The dynamic range of the photoreceptors and pixel circuits, i.e. the region of scene illumination where the sensor produces useful data, spans from under 1lux to more than 10klux¹, whereas the response of the sensor naturally is limited both by the speed of the stimulus and the lighting conditions.

Fig. 6 shows the response of the sensor to the gray dot stimulus moving at different speeds and under different lighting conditions. The discrete levels of illumination were obtained by using a light source which generated 1klux of scene illumination and applying uniform density filters of 1 to 4 decades of attenuation. The dashed line indicates the performance limits of the sensor due to low lighting. At 1lux scene illumination, the dual-line sensor achieves a time resolution that is better than the equivalent time resolution of a conventional line sensor operating at 1000 frames per second (fps). At 10lux, the corresponding time resolution is higher than 10kfps.

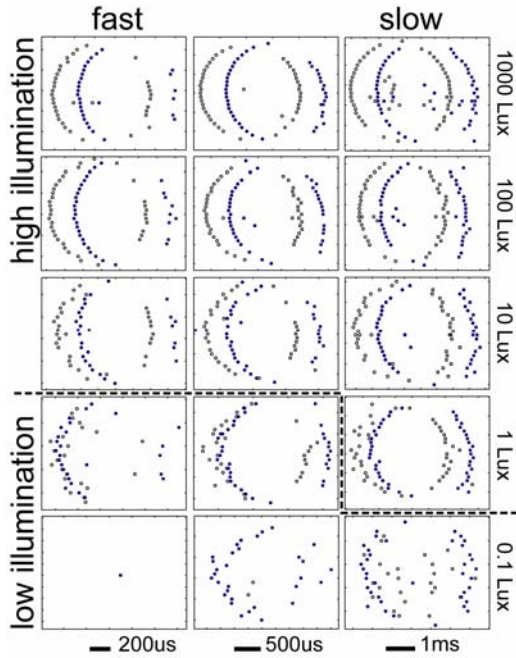


Fig. 6 Plots of the response of the dual-line sensor to described dot stimulus with different illumination conditions and different speeds. The dashed line indicates the low illumination limits of the sensor performance.

C. Application example

Fig. 7 shows the response of the dual-line sensor to a car stimulus in a traffic monitoring scenario. The shift of the second line in respect to the first line is 69ms, corresponding to a speed at the focal plane of 3.47mm/s. Again the delta

¹ Up to now only the lower limit of tolerable scene illumination could be determined experimentally due to the lack of a powerful enough laboratory light source. However the sensor aimed at a scene under bright sunlight, corresponding to a scene illumination of well above 10klux, did not show any signs of malfunction or degradation.

time is best be established by using a correlation method. Knowing the relevant geometrical and optical parameters of the setup, the speed of the car on the road can be calculated from the focal plane speed in a straightforward way. The example car traveled at a speed of 56km/h.

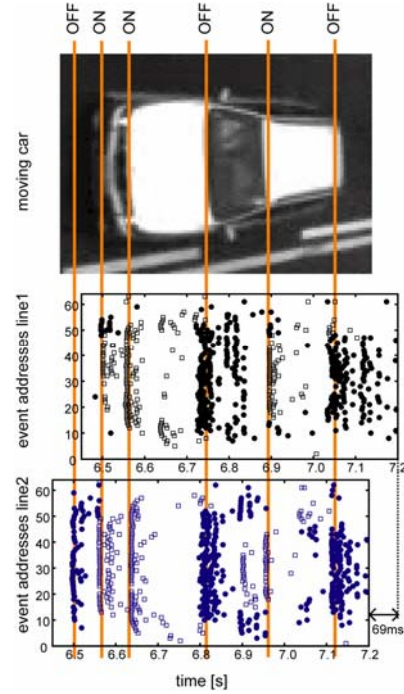


Fig. 7 Plots of the events in time in response to a car moving over the visual field of the lines. The plots are shifted relative to each other and the picture of the car so that ON and OFF edges are aligned.

V. CONCLUSIONS

We described a wide dynamic range dual-line optical sensor for use in compact, low-cost and low-power imaging systems for high-speed measurement applications at varying lighting conditions. Such systems are well suited for use in e.g. traffic monitoring applications as well as industrial applications where target object illumination cannot be controlled.

ACKNOWLEDGMENT

We would like to thank M. Litzenberger and N. Donath for discussions and help with the traffic monitoring data acquisition and evaluation, and K. Boahen, S. Mitra, and G. Indiveri for AER circuit layout.

REFERENCES

- [1] Boahen K., Point-to-point connectivity between neuromorphic chips using Address Events, *IEEE Transactions on Circuits and Systems II: Analog and Digital Signal Processing*, vol. 47 pp. 416-433, 2000.
- [2] T. Delbruck and D. Oberhoff, Self-biasing low-power adaptive photoreceptor, in 2004 International Symposium on Circuits and Systems, ISCAS 2004, pp. IV-844-847, 2004.